

# How does the DNA sequence affect the Hill curve of transcriptional response?

M. Sheinman

*Department of Physics and Astronomy, Vrije Universiteit, Amsterdam, The Netherlands*

Y. Kafri

*Department of Physics, Technion, Haifa 32000, Israel*

(Dated: March 12, 2019)

The Hill coefficient is often used as a direct measure of the cooperativity of binding processes. It is an essential tool for probing properties of reactions in many biological systems. Here we analyze existing experimental data and demonstrate that the Hill coefficient characterizing the binding of many transcription factors to their cognate sites can in fact be larger than one – the standard indication of cooperativity – even in the absence of any standard cooperative binding mechanism. By studying the problem analytically, we demonstrate that this effect occurs due to the disordered binding energy of the transcription factor to the DNA molecule and the steric interactions between the different copies of the transcription factor. We quantify the dependence of the strength of this effect on the different parameters in the problem. In addition, we show that the enhanced Hill coefficient implies a significant reduction in the number of copies of the transcription factors which is needed to occupy a cognate site and, in many cases, can explain existing estimates for numbers of the transcription factors in cells.

PACS numbers:

There has been a large experimental effort [1] to map the binding energy between transcription factors (TFs) in their specific state and different subsequences on the DNA. It is known that to a good approximation the energy can be written as a sum of energies representing the binding energy of a nucleotide on the DNA to the region on the protein with which it is aligned [2, 3]. Specifically, the binding energy of a nucleotide  $s = A, C, G, T$  to position  $j = 1, 2, \dots, L$  (where  $L$  is the length of the protein's DNA binding domain in units of basepairs) is usually described by a  $4 \times L$  position weight matrix (PWM),  $\epsilon_{s,j}$ . By now, the PWM is known for many proteins and, together with a knowledge of the genomic sequence, it specifies the binding energy landscape of TFs to the DNA. Within this framework the binding energy to a specific location on the DNA is a sum of  $L = 10 - 30$  independent variables. Therefore, assuming a pseudorandom sequence on the non-cognate DNA, the probability distribution of the binding energy,  $\Pr(E_i)$ , is close to normal (see [4] and Figs. 1(a) and 2(a)):

$$\Pr(E_i) = \frac{1}{\sqrt{2\pi\sigma^2}} e^{-\frac{E_i^2}{2\sigma^2}}, \quad (1)$$

where we define the centre of the normal distribution as zero energy. The value of  $\sigma$  characterizes the width of the disordered binding energy profile along the DNA and is usually in the range 2–8, where throughout the paper we measure energy in units of  $k_B T$  with  $k_B$  the Boltzmann constant and  $T$  the temperature.

Irrespective of the energy landscape properties, the binding of a TF to an operator—a specific subsequence on the DNA—is typically described by a Hill curve [5]. Namely, if we consider a DNA molecular inside a container representing, say, a prokaryotic cell the occupation

probability of an operator by a TF is given by,

$$P_T = \frac{1}{1 + \left(\frac{m_{1/2}}{m}\right)^n}. \quad (2)$$

Here  $m$  is the number of TFs in the cell and at  $m = m_{1/2}$  the occupation probability is one half (the conversion to concentrations is trivial). The Hill coefficient (HC),  $n$ , governs the steepness of the curve and is widely used to extract qualitative information about the regulation of genes from experimental data [6–9]. In the simplest cases, when there is no cooperative binding involved one expects  $n = 1$ . In the presence of cooperative interactions  $n$  is different than one. For example, in the case of activation by dimers one expects  $n = 2$  if  $m$  is the number of monomers.

The Hill curve, Eq. (2), is directly related to a formulation of the problem using statistical mechanics and the knowledge of the experimentally measured binding energy landscape of the TF to the DNA. To illustrate this we first consider a simple case where: (i) There is no cooperativity associated with the structure of the TF or its binding properties, such that one would naively expects  $n = 1$ . (ii) The probability of the TF to be off the DNA or in a non-specific conformation on the DNA is negligible. Note that by a non-specific conformation we mean one where the TF is on the DNA but does not interact with the bases. This conformation, which typically occurs due to electrostatic interactions, exists on any location along the DNA, including the cognate site. The effects of both simplifications are discussed in detail below). Then, for an operator with energy  $E_T$  the occupation probability is given by

$$P_T = \frac{1}{1 + e^{E_T - \mu}}. \quad (3)$$

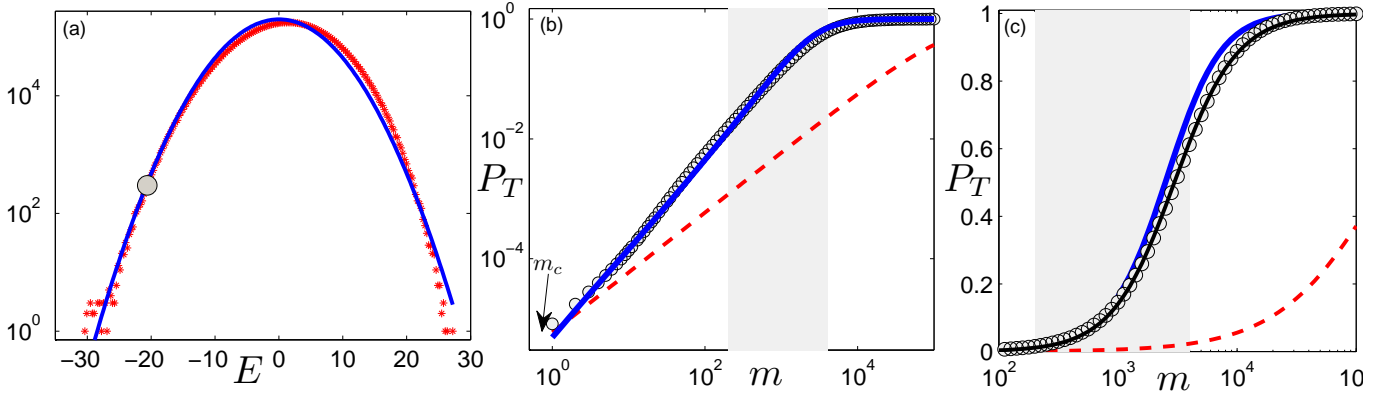


FIG. 1: (a) A histogram of the binding energies of the LexA TF to the *E. coli* genome. The red points represent numerical data while the line is based on a Gaussian fit with  $\sigma = 5.76$ . The big filled circle marks the binding energy to the recQ operon sequence with  $E_T = -20.6$ . (b) The occupation probability of the LexA protein to the recQ operon as a function of  $m$ . The circles represent numerical data based on the PWM of the protein and the *E. coli* DNA sequence. The dashed line is based on the annealed approximation, Eq. (8), while the solid line on Eq. (23). The solid arrow shows the crossover value (nonphysical in this case) of the protein copy number,  $m_c = 0.65$ , predicted by Eqs. (14), and (21). (c) The same data as shown in panel (b) with a Hill function, Eq. (2), fit (thin line) to the numerical data (circles) with  $n = 1.7$  and  $m_{1/2} = 3000$ . The gray areas in (b) and (c) show the typical range of the LexA copy number in *E. coli* (200 – 4000) [14].

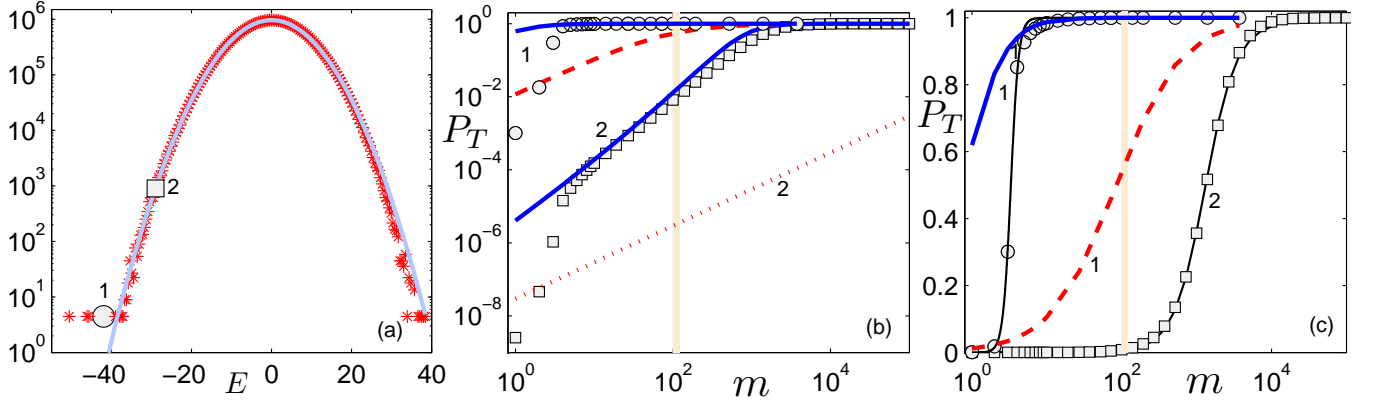


FIG. 2: (a) A histogram of the binding energy of the RpoN TF to the *E. coli* genome. The red points represent the numerical data while the line is based on a Gaussian fit with  $\sigma = 7.8$ . The circle shows the binding energy to the argT operon with  $E_T = -41.8$ . The square shows the binding energy to the fixABCX operon with  $E_T = -28.9$ . (b) The occupation probability of the RpoN protein for the operons argT (circles and 1 symbol) and fixABCX (squares and 2 symbol) as a function of  $m$ . The circles and squares represent numerical data based on the PWMs of the TFs and the *E. coli* DNA sequence. The dashed (dotted) line is based on the annealed approximation, Eq. (8), for the argT (fixABCX) operon, while the solid lines are based on Eq. (23). (c) The same numerical data as in panel (b) with a fit of a Hill function, Eq. (2), (thin, solid, black lines) to the numerical data with  $n = 8.3$  and  $m_{1/2} = 3.3$  for the argT operon and with  $n = 2.07$  and  $m_{1/2} = 1300$  for the fixABCX operon. Vertical areas in panels (b) and (c) show the typical number of the RpoN proteins in *E. coli* ( $\sim 110$ ) [15].

The chemical potential,  $\mu$ , is set by the solution of the equation

$$e^{-F_{ns} + \mu} + \sum_{i=1}^N \frac{1}{1 + e^{E_i - \mu}} = m. \quad (4)$$

Here  $E_i$  is the binding energy of the TF at location  $i = 1, 2, \dots, N$ , with  $N$  the number of accessible DNA binding sites, on the DNA. We assume that different copies of the TF exhibit steric interactions, resulting in

Fermi-Dirac statistics in Eq. (4).  $F_{ns}$  is the free energy associated with a TF in the solution or in nonspecific conformations on the DNA [4, 10–12] and, for now, under our assumption (ii) is negligible. In what follows it will be useful to bear in mind that a non-negligible contribution can only reduce the value of  $P_T$  and enhance  $m_{1/2}$ .

Using Eqs. (3) and (4) it is straightforward to calculate  $m_{1/2}$  and  $P_T(m)$  numerically. We use the PRODORIC database for PWM's of *E. coli* TFs [1], their cognate se-

quences and the genomic sequence of *E. coli* with<sup>1</sup>  $N = 2 \times 4686077$ . First, we evaluate numerically  $m_{1/2}$  for different cognate sites of several proteins. The results are shown in Fig. 3 (for the moment focus on the data shown as circles in panels *a, b* and *c*). As can be seen (and intuitively clear), the weaker the binding energy of the cognate site (larger  $E_T$ ) the larger  $m_{1/2}$ . The values of  $m_{1/2}$  span a large range for different TFs and for different cognate sites of the same TF. Next, in Figs. 1 and 2 (*b* and *c* panels) we present the occupation probability of typical cognate sites for two representative TFs, one cognate site of LexA and two of RpoN. In addition we fit the results to a Hill curve. With the value of  $m_{1/2}$  given the only fit parameter is the HC,  $n$ . Surprisingly, for the three cases (and others not shown) we obtain  $n > 1$  despite the absence of cooperativity in the model (in Figs. 1 and 2 we obtain  $n = 1.7, 8.3, 2.03$ ). These results imply that the DNA sequence and steric interactions between the TF copies can induce a *disorder enhanced HC*. As shown below the enhanced HC occurs when the disorder in the binding energies is so strong that the partition function is dominated by a few very strong binding sites on the DNA. As the number of TFs is increased these sites quickly get occupied. The steric interactions of other TFs with these occupied sites causes the energy landscape experienced by them to be changed significantly. In particular, this implies that their occupation probability increases dramatically leading to an enhanced HC. This is the main results of this paper.

In what follows we show that indeed this is a generic effect related to the disordered binding energy landscape on the DNA. By analyzing the disordered statistical mechanics problem we show that when

$$E_T > -\sigma^2, \quad (5)$$

where  $\sigma^2$  is the variance of the binding energy landscape of the TF to the DNA, the HC is always greater than one and in principle unbounded from above. Moreover, we show that this effect persists as long as the proteins spend most of their time in a specific state on the DNA (see the discussion below for the exact condition). When this is not the case the value of  $m_{1/2}$  grows dramatically, as  $\exp(E_T - F_{ns})$ , making this a rather costly option for many TFs [13]. In fact, as shown below for many of the TFs we consider, data on TF numbers in *E. coli* [14] suggests a value of  $m_{1/2}$  which does not agree with the partition function dominated by  $F_{ns}$ . Finally, we show that when naive considerations give a HC of  $\bar{n}$  the disorder will lead to a HC which is given by  $\bar{n} \cdot n$ , with  $n$  the *disorder enhanced HC* obtained when there is no cooperative binding.

The above results are summarized in Fig. 4 where we plot for several TFs and all their known cognate sites the value of  $E_T + \sigma^2$ . The regime  $E_T + \sigma^2$  smaller/greater than zero corresponds to a without/with disorder enhanced HC. In addition we calculate using data on TF numbers the value of  $E_T + \sigma^2$  which would yield  $P_T = 1/2$  with the typical estimated number of TFs in *E. coli*. As can be seen the numbers indicate that a disorder induced HC is likely for a significant fraction of the TFs and their cognate sites.

To understand these results we first analyze the disordered statistical mechanics problem under our assumptions (i) and (ii). Later we discuss the results when both assumptions are dropped.

Assuming a pseudorandom DNA sequence implies that Eq. (4) is well approximated, for  $N \gg 1$ , by

$$\left\langle \frac{1}{1 + e^{E-\mu}} \right\rangle = \int_{-\infty}^{\infty} \frac{\text{Pr}(E)}{1 + e^{E-\mu}} dE = \frac{m}{N}, \quad (6)$$

where the binding energy probability density is given by Eq. (1) and the angular brackets are defined by the integral.

Before presenting a full analysis of the problem it is interesting to consider a standard *annealed* approximation. Namely,

$$\left\langle \frac{1}{1 + e^{E-\mu}} \right\rangle \simeq \frac{1}{1 + \langle e^{E-\mu} \rangle}. \quad (7)$$

The occupation probability of the cognate sequence in the annealed approximation is then given by

$$P_T^{\text{annealed}} = \frac{1}{1 + \frac{N}{m} e^{E_T + \frac{\sigma^2}{2}}}. \quad (8)$$

Thus, by comparing with Eq. (2) one has

$$m_{1/2} = N e^{E_T + \frac{\sigma^2}{2}}, \quad (9)$$

$$n = 1. \quad (10)$$

In particular, this implies that within the annealed approximations there is no enhanced HC and one obtains the naive results.

From the numerical experiment presented before, clearly, the annealed approximation can fail. In addition to giving a wrong value for  $n$  it gives, in some cases, unreasonable values of  $m_{1/2}$ . Indeed, in Figs. 1 and 2 we show numerical results for LexA compared with Eq. (8). The values of  $m_{1/2}$  differ by more than two orders of magnitude and as stated above the value of  $n$  is larger than one. Moreover, the number of LexA TFs in the cell is estimated to be between 200 to 4000, a value much lower than the  $m_{1/2} = 10^5$  found in the annealed approximation. A similar disagreement between the numerical results and the annealed approximation occurs for the RpoN protein as well as many other TFs.

<sup>1</sup> We assume that all sites are accessible. Otherwise,  $N$  has to be taken as the number of accessible sites. As clear from the discussion below this would only enhance the effects discussed below.

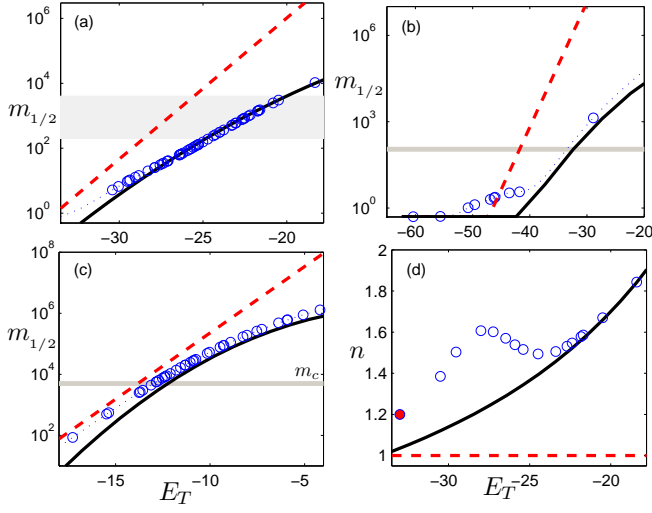


FIG. 3: The value of  $m_{1/2}$  is presented as a function of the energy of different cognate sequences,  $E_T$  for (a) LexA, (b) RpoN and (c) Lrp. The dotted lines are based on a numerical calculation using the *E.coli* genome. The circles represent energies calculated from all known cognate sites of the TF. The black solid lines are based on the freezing regime approximation, Eq. (24), while the red dashed lines are based on the annealed approximation, Eq. (17). Filled, gray horizontal areas show the typical range of the TF's copy number in *E.coli*. The symbol  $m_c$  in (c) marks the crossover value of the Lrp TF between the self-averaging and freezing regimes, predicted by Eqs. (14,21). (d) The HC, obtained by a fit of the numerical data to Eq. 2, is shown as a function of the cognate site energy for the LexA TF. The solid line is the analytical prediction, Eq. (25), while the circles represent numerical data based on real DNA and cognate sites sequence. The filled circle represents the HC of a hypothetical cognate site with a perfect consensus sequence. The dashed line represents the result of the annealed approximation, Eq. (10), which gives  $n = 1$ .

To analyze the problem more carefully we evaluate the integral in Eq. (6) using a saddle point approximation. The resulting set of equations are

$$\mu = E_* + \ln \left( -\frac{\sigma^2}{E_*} - 1 \right) \quad (11)$$

and

$$\frac{e^{-\frac{E_*^2}{2\sigma^2}}}{\sigma^2 \sqrt{\frac{1}{\sigma^2} + \frac{1}{E_* + \sigma^2} + \frac{1}{(E_* + \sigma^2)^2}}} = \frac{m}{N}, \quad (12)$$

where  $E_*$  is the value of  $E$  at the saddle point. Eq. (12) may be solved self-consistently in two limiting cases:

a. *Self-averaging regime:* In this regime the saddle point occurs at  $E_* \simeq -\sigma^2$ , so that Eq. (12) implies

$$E_* = -\sigma^2 \left( 1 - \frac{m}{N} e^{\sigma^2/2} \right). \quad (13)$$

Self-consistency in this regime requires

$$m \ll m_c = N e^{-\frac{\sigma^2}{2}}. \quad (14)$$

The disorder width,  $\sigma$ , has different values for different TFs with typical values in the range of 2 – 8. Thus, the crossover value of the protein's copy number varies from a non-physical  $10^{-7}$  (where the annealed approximation surely fails) to  $10^5$  where the annealed approximation is expected to hold unless the number of TFs is extremely high. The chemical potential (11) in this limit is given by

$$\mu = -\frac{\sigma^2}{2} - \ln \left( \frac{N}{m} \right) \quad (15)$$

and the occupation probability by the same expression given in Eq. (8) so that

$$P_T^{\text{self-averaging}} = \frac{1}{1 + \frac{N}{m} e^{E_T + \frac{\sigma^2}{2}}}. \quad (16)$$

The above derivation implies that the annealed approximation (valid in the self-averaging regime) will give a good estimation of the HC and the number of particles at half occupation,

$$m_{1/2} = N e^{E_T + \frac{\sigma^2}{2}} \quad (17)$$

$$n = 1, \quad (18)$$

only when  $m_{1/2} \ll m_c$ . Furthermore, to be in the self averaging regime near  $m \simeq m_{1/2}$  the cognate site of interest, with energy  $E_T$ , has to satisfy the condition

$$E_T < -\sigma^2. \quad (19)$$

b. *Freezing regime:* In this regime the saddle point satisfies  $|E_*| \ll \sigma^2$  and Eq. (12) implies

$$E_* = -\sigma \sqrt{2 \ln \left( \frac{N}{m \sqrt{1 + 2\sigma^2}} \right)} \quad (20)$$

Self-consistency requires

$$m \gg m_c = N e^{-\frac{\sigma^2}{2}}. \quad (21)$$

The chemical potential in this limit is then given by

$$\mu = -\sigma \sqrt{2 \ln \left( \frac{N}{n \sqrt{1 + 2\sigma^2}} \right)} + \ln \left( \frac{\sigma}{\sqrt{2 \ln \left( \frac{N}{n \sqrt{1 + 2\sigma^2}} \right)}} - 1 \right) \quad (22)$$

and the occupation probability by Eq. (3):

$$P_T^{\text{Freeze}} = \left\{ 1 + \frac{\exp \left[ E_T + \sigma \sqrt{2 \ln \left( \frac{N}{n \sqrt{1 + 2\sigma^2}} \right)} \right]}{\left[ \frac{1}{\sigma} \sqrt{2 \ln \left( \frac{N}{n \sqrt{1 + 2\sigma^2}} \right)} \right]^{-1} - 1} \right\}^{-1}. \quad (23)$$

If close to saturation of the cognate site the system is in the freezing regime (the term freezing is borrowed

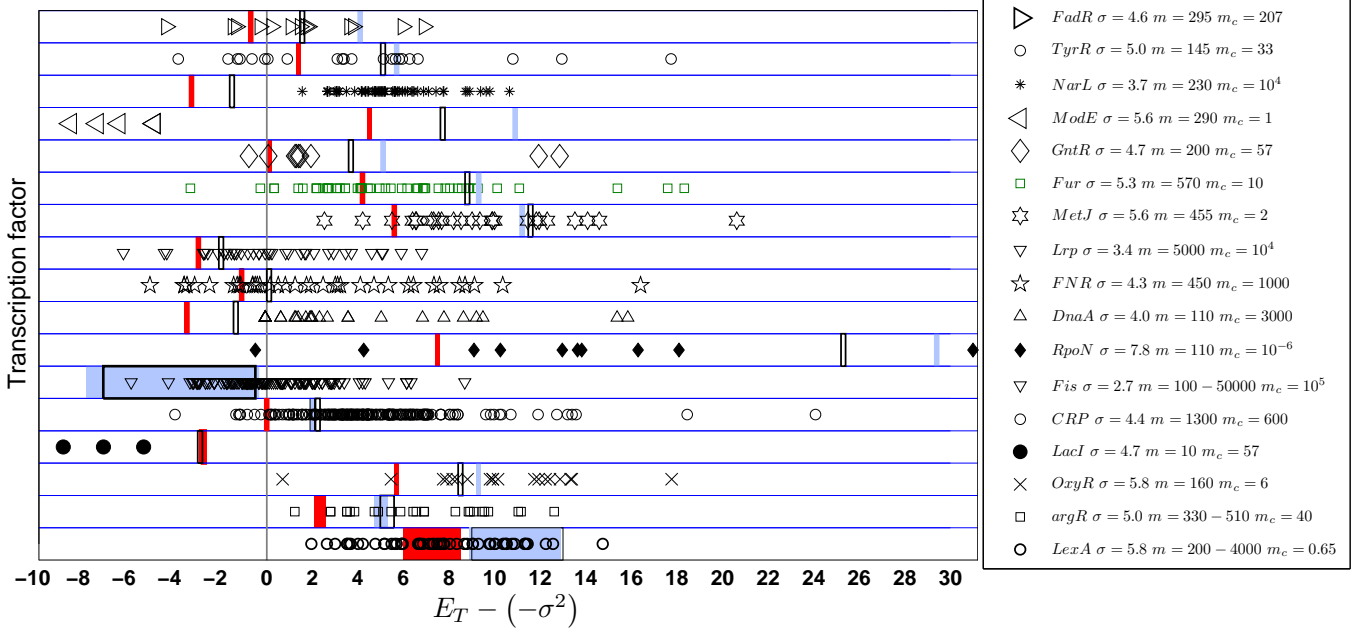


FIG. 4: A classification of cognate sites of different TFs. For each TF (y-axis)  $E_T - (-\sigma^2)$  is plotted for all its known cognate sites (taken from [1]). Empty rectangles represent a hypothetical cognate site's energy that is half-occupied if the number of TFs is as specified in the database [16] (see legend). For TFs with  $m < m_c$  filled red areas represent the same hypothetical energy, as predicted by Eqs. (17). When the typical number of the TFs in the cell is larger than  $m_c$  the hypothetical cognate sites' energies calculated from the annealed approximation (9) are presented by the red filled area while the results of applying Eq. (24) are presented by the blue filled areas.

from similar effects in disordered problems in statistical physics [17]),  $m_{1/2} \gg m_c$ . Then comparing Eqs. (16) and (2) one can see that

$$m_{1/2} = \frac{N}{\sqrt{1 + 2\sigma^2}} e^{-\frac{W^2(e^{-E_T}\sigma^2)}{2\sigma^2}} \quad (24)$$

$$n = \frac{1 + W(e^{-E_T}\sigma^2)}{W^2(e^{-E_T}\sigma^2)} \sigma^2, \quad (25)$$

where  $W$  is the Lambert  $W$ -function [18]. The function is well approximated by  $W(X) \simeq X - X^2$  for small values of  $X$  and by  $W(X) \simeq \ln(X)$  for large  $X$ . Note that to be in the freezing regime close to saturation of the cognate site the condition

$$E_T > -\sigma^2 \quad (26)$$

has to be satisfied.

To check our analytical results we plot both the annealed approximation and the results from the freezing regime in Figs. 1 and 2. The annealed approximation, (8), clearly fails. In contrast Eq. (23) agrees well with the numerical data (strictly the self-averaging result gives a good approximation below  $m_c = Ne^{-\frac{\sigma^2}{2}}$ ). In particular, the HC of the numerical data in the analyzed cases is clearly above one and depends on the disorder width and the cognate site's energy, as demonstrated by Eq. (23).

It is interesting to note that close to saturation the Hill curve (determined by the value of  $m_{1/2}$  and the steepness

of  $P_T$ ) is well described by Eqs. (17), (18), (24), and (25), as presented in Fig. 3. However, in some cases there is a disagreement between the theory and the numerical results for small values of the protein copy number (see the small  $m$  values in Fig. 2(b) and (c) and the low  $E_T$  values in Fig. 3(b) and (d)). This disagreement is due to the deviation of the binding energy probability density from a normal distribution at the low energy tail (see Figs. 1(a) and 2(a)). This effect, which is easy to calculate numerically, increases both the value of  $m_{1/2}$  and  $n$  relative to the analytical predictions. As shown in Fig. 2(a) and (b) in some cases this effect may be significant and lead to a very large HC ( $n = 8.3$  for the argT operon of RpoN). In all the presented cases the annealed approximation clearly fails by several orders of magnitude.

To examine the validity and relevance of these results to other TFs we use a database of 17 known PWMs of TFs of *E. coli*, chosen randomly, and their known binding sites' sequences [1]. Many of the TFs are present in large copy numbers, larger than their  $m_c$  value (see the legend in Fig. 4). Therefore, the annealed approximation of the occupation probability, (8), does not approximate well the occupation probability of many cognate sequences in the biologically relevant regime. In addition, as one can see in Fig. 4, the value of  $E_T + \sigma^2$  for many cognate sites of many proteins is positive. As suggested by Eq. (26), to describe the occupation probability of such cognate sites Eqs. (16), and (23) have to be used, while the annealed



approximation, Eq. (8), fails.

It is instructive to calculate the chemical potential or the value of a hypothetical cognate site energy, denoted by  $\tau$ , which is half-occupied when the number of the TF,  $m$ , is as it is measured in experiments. The results are shown in Fig. 4. One can clearly see that the value of  $\tau$  is smaller (larger) than  $-\sigma^2$  if  $m$  is smaller (larger) than  $m_c$ , as suggested by conditions (19), and (26). Moreover, the annealed approximation predicts well the value of  $\tau$  for  $m < m_c$  but fails for  $m > m_c$  predicting much lower values and, therefore predicting very small occupation probability for all the cognate sites with an energy above  $\tau$ . In contrast, Eqs. (15), and (22) predict well the location of the hypothetical, half-occupied energy for both weak and strong cognate sequences.

The analysis above relied on (i) no inherent cooperativity in the TF, and (ii) a negligible probability to be in non-specific states either on or off the DNA. We now turn to discuss the influence relieving these assumptions. *Effects of cooperativity:* In our study, so far, we ignored the possibility of cooperative effects between distinct molecules of the TF. However, many TFs are active only in their  $\bar{n}$ -meric form. In this case the HC is usually expected to be close to  $\bar{n}$  since the number of active molecules of the TF is proportional to the  $\bar{n}$ 'th power of the concentration of monomers [5]. One can reformulate the above derivation with  $m$  acting as the number of active,  $\bar{n}$ -meric copies of the TF. In this case the HC according to the arguments given above is  $\bar{n} \cdot n$ . Thus, a combination of cooperativity and quenched disorder can naturally lead to a high values of the HC.

*The effect of nonspecific states:* In our study, so far, we ignored nonspecific states of the protein. These states exist and correspond either to the TF being in the solution or in a nonspecific conformation bound to the DNA [4, 10–12]. Namely, the nonspecific free energy is given by

$$F_{ns} = \ln(e^{-E_{3D}} + Ne^{-E_2}), \quad (27)$$

where  $E_{3D}$  is the free energy of an unbound TF (modeled say by the free-energy of a solution of TFs) and  $E_2$  is the energy of the bound protein in the nonspecific conformation which for simplicity we assume to have the same energy for all sites along the DNA (the results are unchanged, being proportional to  $N$ , in the presence of small disorder in this binding energy with a slight reinterpretation of  $E_2$ ). Clearly, these nonspecific states can only reduce the occupation probabilities of the cognate sites calculated in Eqs. (16) and (23). However, as suggested previously the existence of these nonspecific states can be an important component for the dynamics of the search and recognition process carried out by the TF [4, 10, 11, 19].

From Eq. (4) one can see that the nonspecific energy is negligible when

$$F_{ns} \gg \mu + \ln m. \quad (28)$$

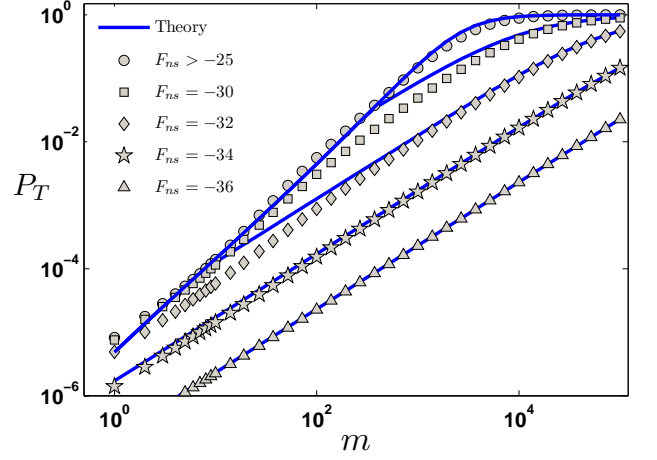


FIG. 5: The occupation probability of the LexA TF to one of its cognate sequences, the recQ operon, is presented for different values of the nonspecific energy. Different symbols represent the numerical data (see legend) while the solid curves are based on Eq. (29).

Otherwise a significant fraction of the TFs are in the nonspecific state so that the chemical potential is well approximated by  $F_{ns}$ . Thus, the occupation probability of the cognate site may be approximated by

$$P_T = \min \left( \frac{1}{e^{E_T - \mu} + 1}, \frac{1}{\frac{e^{E_T - F_{ns}}}{m} + 1} \right), \quad (29)$$

where  $\mu$  is given by Eqs. (16), and (23). In Fig. 5 we show that indeed this results agree well with the numerical calculations for different values of the nonspecific energy. Thus, condition (28) implies that a half occupation of the cognate site occurs in the freezing regime (so that  $n > 1$ ) if

$$F_{ns} \gg E_T + \ln m_{1/2}. \quad (30)$$

Since we are not aware of direct measurements of the nonspecific binding it is hard to estimate if this condition holds. We do stress, however, that the experimentally measured numbers of TFs in the cell suggest that it does not play an important role for many TFs.

In sum, the nonspecific states may be ignored if most of the TFs are mostly bound to the DNA in a specific conformation. Otherwise the chemical potential takes a value which is closer to the nonspecific free energy. This causes the occupation probability to be well approximated by the annealed approximation which results in a Hill curve with  $n = 1$  and  $m_{1/2} = e^{E_T - F_{ns}}$ . However, in many cases the free energy of the nonspecific states which is needed to bring the system to the self averaging regime is very low. Then the cognate site is significantly occupied only if the number of TFs is much larger than its typical value in the cell. In Fig. 6 the parameters of the Hill curve are shown for different values of  $F_{ns}$ . One can see that

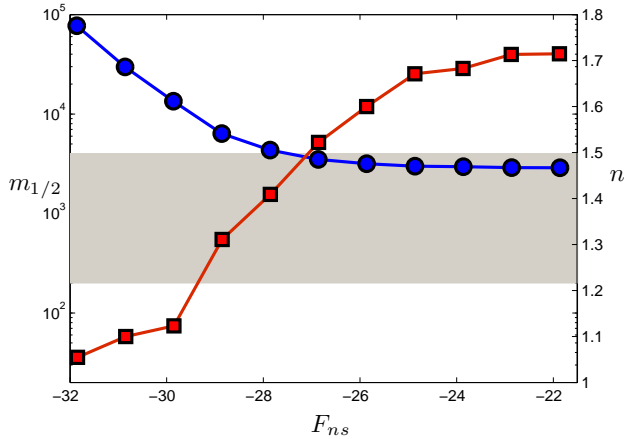


FIG. 6: The parameters of the fitted Hill curve, Eq. (2), are presented for the occupation probability of the LexA TF to one of its cognate sequences, the recQ operon as a function of the nonspecific free energy. The circles represent  $m_{1/2}$  while the squares represent  $n$ . The filled gray horizontal area shows the typical range of the LexA copy number in *E. coli* (200 – 4000) [14].

to decrease the HC to one, the value of  $m_{1/2}$  has to be much larger than the typical copy number of the protein. Note, that even in this case the occupation probability might scale as  $m^n$  with  $n > 1$  far from the saturation regime,  $m_c \ll m \ll \exp(F_{ns} - \mu)$  (see Fig. 5, for an example). In fact the existence of the nonspecific states can totally eliminate the disorder induced HC for all values of  $m$  only if the condition  $F_{ns} \ll \mu + \ln m_c$  is satisfied.

*Summary* The considerations discussed in this paper suggest the existence of a disorder enhanced HC. They provide an estimate of the TF's copy number needed to significantly occupy its cognate sites. This estimate is shown in many cases to be much smaller and more consistent with the existing data than a naive estimate, based on the annealed approximation. This study was performed using the measured PWMs of several TFs and can easily be extended to others.

### Acknowledgments

We acknowledge useful comments from A. Horovitz, R. Voituriez, O. Benichou, L. Mirny, E. Braun, A. Sharma and M. Depken. M.S. thanks FOM/NWO for financial support.

- 
- [1] R. Munch, K. Hiller, H. Barg, D. Heldt, S. Linz, E. Wingender, and D. Jahn, Nucl. Acid. Res. **31**, 266 (2003).
  - [2] O. G. Berg and P. H. von Hippel, J. Mol. Biol. **193**, 723 (1987).
  - [3] G. Stormo and D. Field, Trends Biochem. Sci. **23** (1998).
  - [4] M. Slutsky and L. A. Mirny, Biophys. J. **87**, 4021 (2004).
  - [5] R. Phillips, J. Kondev, and J. Theriot, *Physical biology of the cell* (Taylor and Francis, New York, 2009).
  - [6] N. E. Buchler, U. Gerland, and T. Hwa, Proc. Nat Acad. Sci. USA **102**, 9559 (2005).
  - [7] T. Kuhlman, Z. Zhang, M. H. Saier, and T. Hwa, Proc. Natl Acad. Sci. USA **104**, 6043 (2007).
  - [8] H. D. Kim, T. Shay, E. K. O'Shea, and A. Regev, Science **325**, 429 (2009).
  - [9] H. G. Garcia, A. Sanchez, T. Kuhlman, J. Kondev, and R. Phillips, Trends in Cell Biology **20**, 7233 (2010).
  - [10] O. G. Berg, R. B. Winter, and P. H. von Hippel, Biochem. **20**, 6929 (1981).
  - [11] U. Gerland, J. D. Moroz, and T. Hwa, Proc. Natl. Acad. Sci. USA **99**, 12015 (2002).
  - [12] C. G. Kalodimos, N. Biris, A. M. J. J. Bonvin, M. M. Levandoski, M. Guennuegues, R. Boelens, and R. Kaptein, Science **305**, 386 (2004).
  - [13] G.-W. Li, O. G. Berg, and J. Elf, Nature Phys. **5**, 294 (2009).
  - [14] A.-M. Dri and P. L. Moreau, Mol. Microbiol. **12**, 621 (1994).
  - [15] M. Jishage, A. Iwata, S. Ueda, and A. Ishihama, J. Bacteriol. **178**, 5447 (1996).
  - [16] Y. Ishihama, T. Schmidt, J. Rappsilber, M. Mann, F. U. Hartl, M. Kerner, and D. Frishman, BMC Genomics **9**, 102 (2008).
  - [17] B. Derrida, Phys. Rev. Lett. **45**, 79 (1980).
  - [18] M. Abramowitz and I. Stegun, *Handbook of mathematical functions with formulas, graphs, and mathematical tables* (Dover Publications, Incorporated, 1970).
  - [19] M. Sheinman, O. Bénichou, Y. Kafri, and R. Voituriez, ArXiv e-prints (2011), 1104.0910.